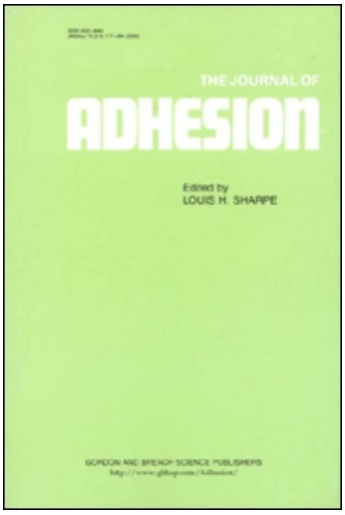

The Journal of Adhesion
Publication details, including instructions for authors and subscription information:
http://www.informaworld.com/smpp/title~content=t713453635

Stick-Slip: Wet Versus Dry

F. Wu-Bavouzet[a]; J. Clain-Burckbuchler[a]; A. Buguin[a]; P. -G. De Gennes†[a]; F. Brochard-Wyart[a]
[a] Institut Curie, Centre de Recherche, Université Paris 6, CNRS UMR 168, Paris, France

To cite this Article Wu-Bavouzet, F. , Clain-Burckbuchler, J. , Buguin, A. , De Gennes†, P. -G. and Brochard-Wyart, F.(2007) 'Stick-Slip: Wet Versus Dry', The Journal of Adhesion, 83: 8, 761 — 784
To link to this Article: DOI: 10.1080/00218460701586178
URL: http://dx.doi.org/10.1080/00218460701586178

The Journal of Adhesion, 83:761–784, 2007

ISSN: 0021-8464 print/1545-5823 online
DOI: 10.1080/00218460701586178

Taylor & Francis
Taylor & Francis Group

Stick-Slip: Wet Versus Dry

F. Wu-Bavouzet
J. Clain-Burckbuchler
A. Buguin
P.-G. De Gennes[†]
F. Brochard-Wyart
Institut Curie, Centre de Recherche, Université Paris 6, CNRS UMR 168, Paris, France

A rubber lens (polydimethylsiloxane) is pressed against silanated or bare glass plates (Johnson-Kendall-Roberts (JKR) contact). As the plate slides with a velocity U, we measure the friction on the lens using a "macro Atomic Force Microscope (AFM)", where the cantilever is a thin rectangular glass rod and the tip is the rubber lens. We observe the contact area via optical interferometry.

In air for "hard" lenses (Young's modulus $E \approx 1\,MPa$), we find smooth sliding on a model substrate, and a transition to stick-slip on a hysteretic substrate above a threshold velocity, V_M. For soft lenses ($E \approx 0.1\,MPa$), we observe Schallamach waves and stick-slip depending on normal force and the plate's velocity, U. When immersed in a liquid (silicone oils, water-glycerol mixtures), the contact remains dry at low velocities, but is invaded by a liquid film above a critical velocity, U_c. For hard lenses we observe smooth sliding and high friction below U_c, and low friction above U_c. For soft lenses, we find wet Schallamach waves for $U < V_M$ and stick-slip instabilities at large velocities. In the stick-slip regime, the contact is wet in the slip phase, and dewets in the stick phase. We measure the period of the stick-slip cycle as a function of the liquid viscosity.

We interpret the stick-slip process by the formation and rupture of adhesive bonds (between the rubber polymer chains and active sites on the glass). Using a recent model, we can explain most of the data for the stick-slip period and slip threshold velocity.

Keywords: Lubrication; Rubber/solid friction; Sliding instabilities; Stick-slip

[†]Deceased.

Received 1 February 2007; in final form 20 June 2007.

One of a Collection of papers honoring Liliane Léger, the recipient in February 2007 of *The Adhesion Society Award for Excellence in Adhesion Science, Sponsored by 3m*.

Address correspondence to Francoise Brochard-Wyart, Institut Curie, Centre de Recherche, CNRS UMR 168, Université Paris 6, F75248 Paris, France. E-mail: Francoise-brochard-wyart@curie.fr

NOMENCLATURE

F_n, F_t	normal, tangential forces
F_{t0}	rupture force
a	contact radius
A	contact area
U	glass plate velocity
v	rubber sliding velocity
$\sigma(v)$	shear stress of the sliding lens $\sigma(\mathrm{v}) = F_t/A$
ζ	friction coefficient
V_M	velocity corresponding to a maximum of $\sigma(\mathrm{v})$
V_m	velocity corresponding to a minimum of $\sigma(\mathrm{v})$
E	rubber lens Young's modulus
W	adhesion energy
W_{on}, W_{off}	advancing, receding adhesion energy
$\mathrm{S} = \gamma_{\mathrm{SR}} - (\gamma_{\mathrm{SL}} - \gamma_{\mathrm{LR}})$	liquid, L, spreading parameter at soft interface solid, S, rubber, R
γij	interfacial tension
R	curvature radius of the rubber lens
U_c	forced wetting velocity
η	liquid viscosity
η_0	monomer viscosity
h_0	elastic length
K	spring constant of the adhesive lens ($K = 16\,Ea/9$)
θ	contact angle
θ_{A}, θ_{R}	advancing, receding contact angles
ν	density of adhesive bonds
τ_{on}	healing time
τ_{R}	Rouse time of reticulated polymer chains
τ_0	microscopic relaxation time
l	maximum extension of bond at rupture
$V_c = l/\tau_{on}$	critical unbinding velocity
V_{tip}	crack tip velocity
V_s	slip velocity
σ_0	static rupture stress
F_c	static rupture force
f_χ	bond rupture force
U_b	bond binding energy
w, t, L	cantilever dimensions

1. INTRODUCTION

The friction of rubbers on dry or wet solid substrates is clearly of major practical importance and has been studied in considerable detail for engineering purposes [1–6]. However, there is still a lack of understanding of the various slippage regimes observed, and the new features when the rubber in air is immersed in a liquid. We present here:

- Some new experiments with controlled mechanical conditions;
- Comparisons with a simple theoretical model.

We concentrate on the case of polydimethylsiloxane (PDMS) rubbers in contact with:

- A silanated substrate;
- A poorly silanated substrate, where holes in the molecular carpet give rise to local strong adhesion and hysteresis;
- Bare glass, which is chemically heterogeneous.

We use hard and soft rubber lenses, of Young's modulus $E \approx 1\,\text{MPa}$ and $E \approx 0.1\,\text{MPa}$, respectively. The mechanical conditions (Figure 1) are an adaptation of the classical test analyzed long ago by Johnson, Kendall, and Roberts (JKR) [7]. The rubber is a flat/convex lens (of

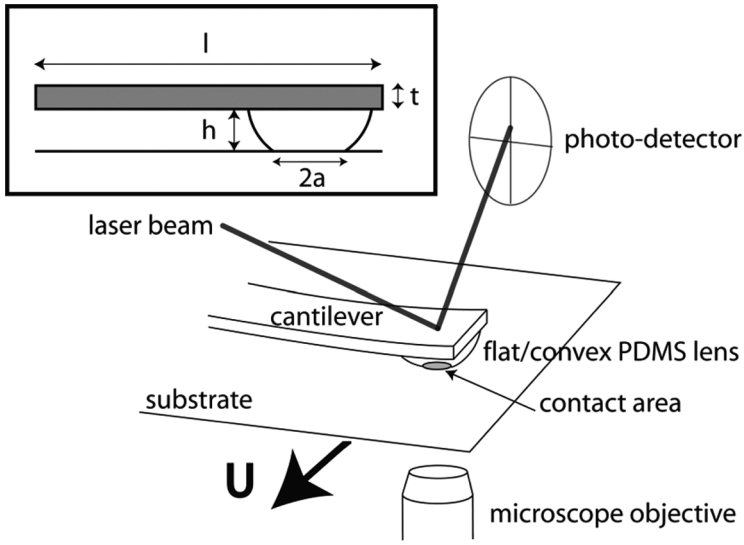

FIGURE 1 Experimental set-up. The PDMS lens is pressed against the substrate, which moves at velocity U. The contact is observed with a microscope.

radius $R \approx 1\,\mathrm{mm}$) squeezed against the flat support by a normal force, F_n; we monitor the contact radius, a, by optical interference microscopy. Let us first recall the basics for static experiments (no sliding):

- In ideal conditions, the adhesive energy, W (energy per unit contact area), is the same for loading or unloading. Using the JKR theory [7], we can extract from the plots $a(F_n)$, the energy, W, and the Young's modulus, E, of the rubber.
- In many practical cases we must distinguish a W_{on} (for loading processes) and a W_{off} (for unloading processes).

We have performed these experiments with our lenses in both the "dry" and "wet" conditions (in the latter case the lens is immersed in a liquid). For hard lenses on a silanated glass plate, we find $W_{off} = W_{on}$, but hysteresis appears on poorly silanated or bare glass substrates. For soft lenses we see hysteresis on all substrates, with two contributions: one coming from rubber chains "zipping off" the solid surface, and one related to silanisation defects on the glass plate.

Let us now turn to sliding experiments, where we impose a slippage velocity at the glass/lens interface, by moving the glass plate at velocity, U (Figure 1), and measuring the tangential force, F_t.

Our aim is to characterize different sliding modes (smooth/unstable) *versus*:

- The nature of the substrate;
- The softness of the rubber;
- The squeezing force, F;

for dry contacts and for contacts immersed in a liquid.

For dry contacts, we shall define a characteristic velocity, V_M, associated with a transition between steady and unstable (stick-slip) sliding.

In a liquid (water, water-glycerol mixtures, fluorinated silicone oils), we expect similar regimes, plus a wetting transition at $U > U_c$, where a liquid invades the contact. This film lubricates the contact and the friction coefficient, $\mu = F_t / F_n$, drops by a factor of order ten [8]. The scaling law for U_c is [9] $U_c \approx W/\eta(h_0/R)^{1/3}$, where η is the liquid viscosity, h_0 is the elastic length [7] ($h_0 = W/E$), and R is the lens radius. U_c results from a competition between U (forced wetting) and the natural dewetting of the liquid film. By tuning U_c through the viscosity of the liquid we shall expect different successive regimes:

- For $V_M < U_c$, smooth sliding/stick-slip/lubrication;
- For $V_M > U_c$, smooth sliding/lubrication.

Our aim here is to compare the sliding of the rubber lens in air, and immersed in a liquid. We shall focus on the stick-slip sliding instabilities, which can be coupled to wetting and dewetting of the contact if the slip velocity becomes larger than U_c. We first describe the experimental set-up and the fabrication of rubber lenses, the surface treatments, and their characterization. Then, we study and interpret slippage in air. In the last section, we describe the characteristics of sliding in a liquid. We extend the model of stick-slip of lenses in air to lenses in liquid, where wetting and stick-slip are coupled.

2. MATERIAL AND METHODS

The elastomer used for the flat/convex lenses is polydimethylsiloxane (PDMS 170, Dow Corning Corp., Midland, USA) supplied in two liquid parts. Part A contains vinyl endcapped oligomeric PDMS chains: part B consists of a cross linker and a catalyst for the reticulation reaction. Millimetric droplets of A50:B50 and A85:B15 mixtures (w/w) are deposited on a silanated glass slide, and then cured for 48 h at 65°C. The Young's moduli, E, for hard (A50:B50) and soft (A85:B15) flat/convex lenses are 1 MPa and 0.1 MPa, respectively, estimated from JKR tests, or measured directly by compression of a PDMS cylinder, which gives for a hard lens, a Young's modulus value $E \approx 1$ MPa.

The substrates used are:

- A silanated microscope glass slide (SIT84, ABCR, Karlsruhe, Germany), obtained by grafting a monolayer of octadecyltrichlorosilane onto the surface following a classical procedure [10,11];
- A poorly silanated microscope glass slide. Atomic Force Microscope (AFM) images [12] show holes in the dense molecular silane layer of size 100 nm;
- A bare glass slide. This high energy surface is rapidly contaminated by aerosols, which should lower its surface energy.

We have characterized these substrates by the measurement of advancing and receding contact angles, $\Delta\theta = \theta_A - \theta_R$ of clean water droplets. We find $\Delta\theta = 16 \pm 3^\circ$ on silanated glass ($\theta_A = 112^\circ \pm 2^\circ,\ \theta_R = 96^\circ \pm 2^\circ$) and $\Delta\theta = 30 \pm 3^\circ$ on poorly silanated or bare glass (for a poorly silanated surface, $\theta_A = 93^\circ \pm 2^\circ$, $\theta_R = 63^\circ \pm 2^\circ$). This contact angle hysteresis is due to the chemical defects (adhesive patches) [12] and is used as a quality test of surface treatments [13]. The silanated glass ($\Delta\theta < 20^\circ$) is characterized by a small hysteresis whereas for "poorly silanated" glass $\Delta\theta > 20^\circ$.

The liquids used are:

- Water-glycerol mixtures leading to high adhesion energies as in air. We vary the water mass proportions (95% (kinematic viscosity,

$\nu = 1.1$ cS, optical index n = 1.34), 80% ($\nu = 1.7$ cS, n = 1.36), 20% ($\nu = 50$ cS, n = 1.44) and 4% ($\nu = 624$ cS, n = 1.47). Mixtures of optical index close to the PDMS index (1.40) have not been used because the contact cannot be observed;

- Fluorinated silicone oils [polyfluoromethylalkylsiloxane (PFAS), ABCR, Karlsruche, Germany], leading to low adhesion energies. We can vary the viscosities from 80 cS to 10,000 cS, depending on molecular weight.

The experimental set-up is shown in Figure 1. The contact between the silanated glass slide and the PDMS lens immersed in the liquid is observed by reflection interference contrast microscopy (RICM) (microscope Axiovert 135, Zeiss, Le Pecq, France). The interference fringes are clearly visible, and give a measurement of the contact radius, a (Figure 1), and the lens profile. Typical size for a is about 50 μm, measured with a resolution of 2 μm.

The PDMS lens is pressed against the solid substrate with a normal force, F_N, which is maintained constant *via* a piezoelectric crystal. The microscope glass slide lays on a motorized stage (continuous current motor, 860A-2, Newport, Irvine, USA). Sliding is imposed by the translation of the stage with respect to the PDMS lens, which stays at rest in the laboratory reference frame. The sliding velocity is measured by an optical sensor (Renishaw, Wotton-Under-Edge, UK) and ranges from 100 to 800 μm s.

Our home-made force apparatus [8] to measure the normal and tangential forces, F_n and F_t, applied to the lens is similar to an AFM. The PDMS lens (the tip) is stuck under a cantilever which is a thin glass fibre of dimensions 20 mm × 1 mm × 200 μm. A laser diode reflects on the cantilever covered with a thin gold layer (50 nm), and points on a four-quadrant photo-detector.

A normal force leads to a cantilever bending and, consequently, to a vertical deflection of the laser beam. Similarly, when a tangential force is exerted on the PDMS lens, the cantilever twists and the laser beam is deflected horizontally.

A data acquisition interface (Keithley, Cleveland, USA) records the sliding velocity, the piezoelectric crystal voltage, and the photo-detector output signals. The latter gives the normal and tangential forces with two calibrations.

The output signal is proportional to the laser beam deflection on the quadrants, and, thus (for normal forces), to the vertical displacement, Δz, of the cantilever extremity. Once the proportionality coefficient between photo-detector voltage and Δz is measured, the normal force, F_n, is derived from the cantilever stiffness: $F_n = k_n \Delta z$. The coefficient k_n

is measured by the dynamic Cleveland method [14] in air, but remains the same in the liquids used (as it only depends on the cantilever dimension and material). Similarly, for the tangential forces, we measure the proportionality coefficient between photo-detector voltage and the cantilever twist, and the stiffness, k_t, is given by: $k_t = k_n(5/9)(L/(h + t/2))^2$, where h is the lens thickness (see Figure 1), and L and t are the cantilever length and thickness, respectively [15,16]. Typically, $k_n = 10\,\mathrm{N \cdot m^{-1}}$ and $k_t/k_n \approx 800$ for millimetric lenses. The ranges of force obtained are of the order of 100 μN for F_n and 1–100 mN for F_t.

Before each sliding experiment, we perform a JKR test. It consists of a discrete loading/unloading cycle of the lens, which is performed by steps of 2.5 μN. The contact radius, a, and the normal force, F_n, applied on the lens are measured at each step. We wait one minute between two steps to be sure that the system reaches its equilibrium state. We deduce the Young's modulus; E, and the adhesion energy, W, for the lens by using the JKR relation:

$$\frac{a^{3/2}}{R} = \frac{1}{16E/9} \cdot \frac{F_n}{a^{3/2}} + \left(\frac{6\pi W}{16E/9}\right)^{1/2}, \qquad (1)$$

where for compression $W = \mathrm{W}_{on}$, and for decompression $W = \mathrm{W}_{off}$. The slope of $a^{3/2}/R$ *versus* $F_n/a^{3/2}$ yields E and the extrapolation to zero force gives W. The results of several JKR tests for hard lenses, compressed on a silanated substrate in air (see Figure 2a) and in fluorinated oil give $E = 0.95 \pm 0.05\,\mathrm{MPa}$ and $W_{on} = 42 \pm 1\,\mathrm{mN/m}$ in air and $W_{on} = 4.7 \pm 0.8\,\mathrm{mN/m}$ in oil. For a soft lens we find $\mathrm{E} = 0.10 \pm 0.05\,\mathrm{MPa}$ and the same values for W_{on}.

For a hard lens on a silanated substrate, the compression and decompression curves are superimposed: $W_{off} = W_{on}$ (see Figure 2a) whereas, in the case of the same lens on a poorly silanated surface, we observe hysteresis (see Figure 2b), with $W_{off} - W_{on} = 30\,\mathrm{mN/m}$. We also have hysteresis for a soft lens on a silanated substrate.

Hysteresis can have several origins:

- Adsorption of rubber chains on active sites of the substrate—bonds created during the compression phase between the two surfaces do not modify significantly the adhesion energy, W_{on}, but lead to a higher unbinding energy, because energy is lost in the stretching of these bonds before rupture;
- Free chains extraction—surface chains of the lens can interact with the substrate [17,18]. During the decompression, they will be extracted to return to their original position. This costs energy;
- Bulk dissipations in the lens during the decompression phase for soft rubbers.

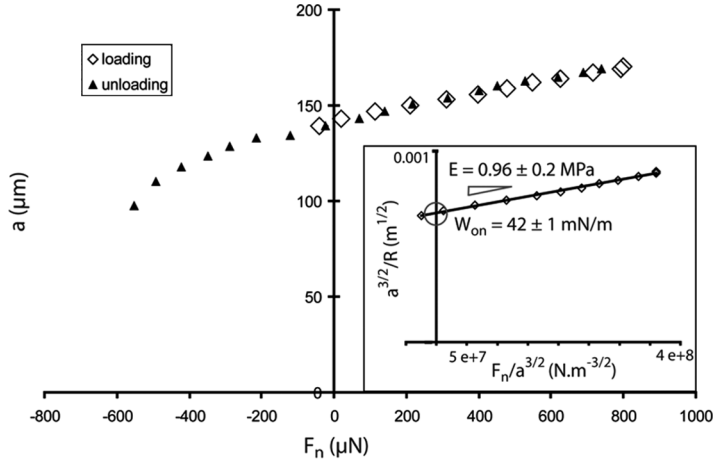

(a)

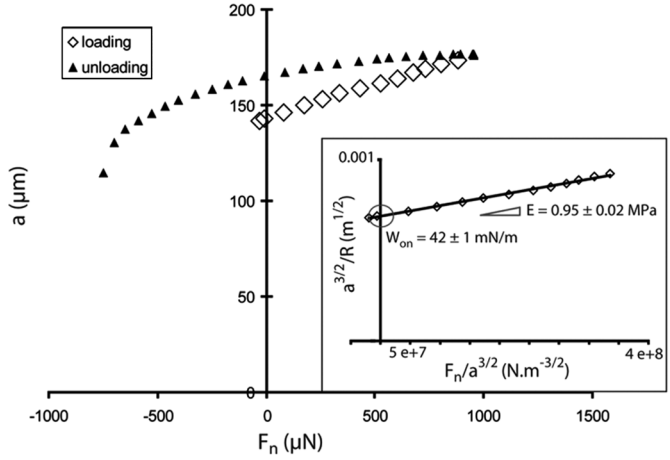

(b)

FIGURE 2 (a) Hard lens on silanated glass in air. *a versus* F_n during a JKR test; no hysteresis is observed. The loading and unloading curves are superimposed; plotting $a^{3/2}/R$ *versus* $F_n/a^{3/2}$ yields E and W_{on}. (b) Hard lenses on a poorly silanated substrate in air; we observe hysteresis.

3. SLIDING OF RUBBER LENSES IN AIR

We study the friction of hard and soft lenses on three types of substrate: silanated, poorly silanated, and bare glass slides. Two parameters (normal force and sliding velocity) have been varied.

3.1. Friction on Model Substrates: Hard Lenses

With hard lenses on silanated slides no hysteresis is observed in JKR tests. During a sliding experiment, the normal force is applied using a piezoelectric crystal and we move the glass plate at velocity U. The tangential force and the lens position are recorded. From the latter, we derive the sliding velocity v of the rubber lens on the substrate.

3.1.1. Contact Observation During Sliding

When the sliding starts at time $t = 0$ s, the contact sticks on the substrate (see Figure 3a, for $U = 430\,\mu\text{m/s}$). At $t = 240$ ms, corresponding to a displacement of about ten micrometers, the contact area, A, decreases and becomes approximately an ellipse, whereas the lens slides smoothly on the glass: in steady state, the sliding velocity, v, of the lens is equal to the substrate velocity U. When the substrate slides slowly, the contact keeps its original circular shape: it follows the JKR laws. As the velocity U increases, the contact area becomes smaller. This effect is mostly visible at low normal loads and is explained by Vorvolakos [19] by a progressive loss of adhesive interactions, and a transition from JKR adhesive to Herzian non-adhesive behaviour. To test this hypothesis, an equivalent radius, $\tilde{a}$, is defined by $A = \pi\tilde{a}^2$. Figure 4a shows the plot of $\tilde{a}^{3/2}$ *versus* $F_n/\tilde{a}^{3/2}$. The plots for different velocities have the same slopes as expected, leading to a measure of $E \approx 0.9$ MPa. The extrapolation to zero force gives the effective adhesion energy, W, *versus* velocity U (see Figure 4b).

This decrease of the effective adhesion energy with velocity may have at least two sources:

- A decrease of the binder density, ν, discussed later. $W = \nu U_b$ with fixed U_b and $\nu(U) = \nu_0/(1 + (U/V_c)) \approx \nu_0(1 - (U/V_c))$. We get from Figure 4b, $V_c = 1.2$ mm/s;
- The application of a tangential force also leads to a decrease of the static contact area. However, a calculation by Savkoor (for a static force) does predict only small changes in the contact area [20].

3.1.2. Tangential Stress $\sigma(U)$

The tangential stress $\sigma(U) = F_t/A$ increases linearly with U (Figure 5a). $\sigma(U)$ discussed in Sec. 4 has two contributions associated to the rupture of molecular bonds and to passive friction. It can be written as $\sigma = \sigma_0 + \zeta U$ in the limit of small binding density. Experimentally, we find on silanated glass $\sigma_0 = 5$ kPa and $\zeta = 10^8$ Pa · s/m. σ_0 is proportional to the density ν_0 of binders and to the force of $fc \approx kT/D$ to break a bond (kT is the thermal agitation, D a molecular length).

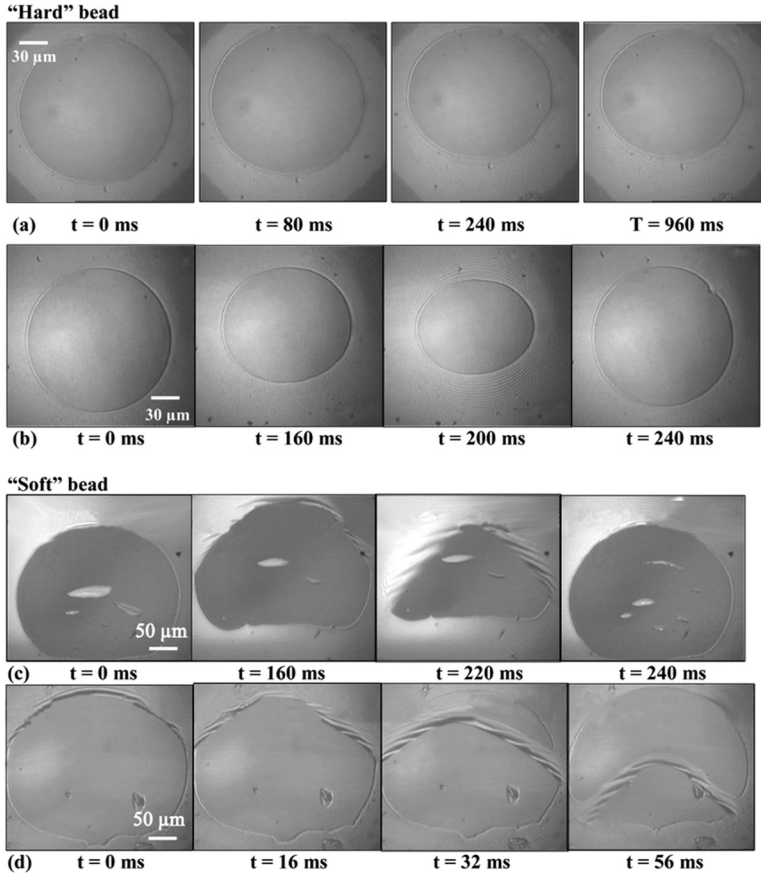

FIGURE 3 (a) Smooth sliding of a hard lens on silanated glass in air. The sliding velocity is $U = 430\,\mu$m/s and the normal force applied on the lens is $F_n = 430\,\mu$m/s. The substrate slides from the bottom to the top. (b) Stick-slip of a hard lens on a poorly silanated substrate in air. (c) Stick-slip of a soft lens on a poorly silanated substrate in air. (d) Schallamach wave propagation in air (soft bead on a poorly silanated substrate). The sliding velocity U is $380\,\mu$m/s and the normal force F_n is $360\,\mu$N.

With $D > lnm$, we find $\sigma_0 > 10^{12}\,\mathrm{m}^{-2}$. Our value for ζ is comparable with the friction coefficient measured by Bureau on PDMS grafted Si wafers [21]. There are two contributions to ζ associated with viscous losses in the rubber sliding on microscopic asperities [5], and molecular friction of polymer chains bound to active sites [21].

We shall see now that on a poorly silanated glass, or bare glass, ν_0 is much larger. In this limit, one must include the progressive

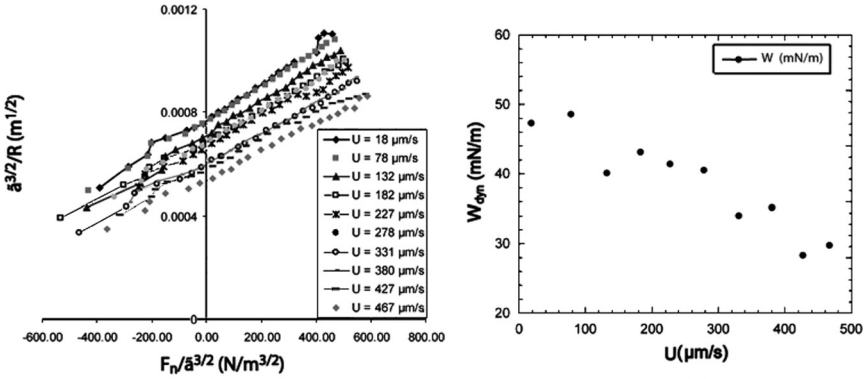

FIGURE 4 Hard lenses sliding smoothly on a silanated substrate: (a) Variations of $\tilde{a}^{3/2}/R$ in function of $F_n/\tilde{a}^{3/2}$ in air. The plots for different velocities have the same slope. (b) Adhesion energy W_{dyn} *versus* sliding velocity U in air.

detachment of binders $\nu = \nu_0/(1 + U/Vc)$ (equations 5 and 6). $\sigma(U)$ becomes a decreasing function of U, leading to stick-slip instabilities.

3.2. Friction on Hysteretic Substrates

The two types of lenses (hard and soft) have been used. The experiments lead to various sliding behaviours (see Table 1), including stick-slip instabilities [22] and Schallamach waves [23].

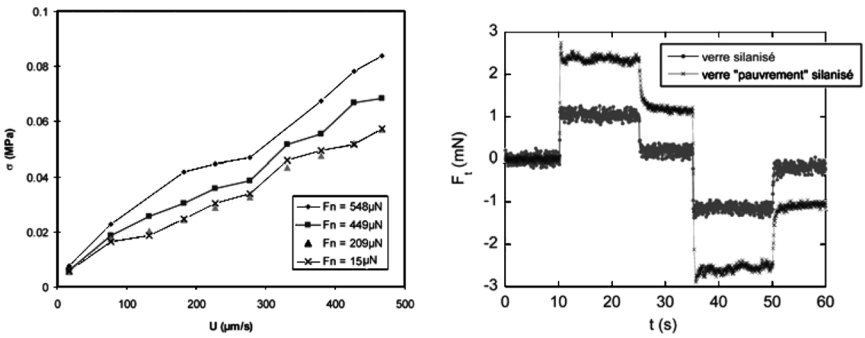

FIGURE 5 (a) Variations of the stress σ_t *versus* sliding velocity U in air. (b) Tangential force F_t for smooth sliding on silanated and poorly silanated substrates in air. The normal force F_n is 380 µN and the sliding velocity U is 270 µm/s.

TABLE 1 Friction Regimes Observed for Hard and Soft Lenses on Different Substrates in Air

Substrate	"Hard" bead → Decreasing crosslinker proportion → "soft" bead
Silanated glass	Sliding → Sliding/stick-slip
Poorly silanated glass	Sliding/stick-slip → Waves/stick-slip
Bare glass	Stick-slip → Waves/stick-slip

3.2.1. Hard Lenses

We describe now the sliding of the same hard lens on a substrate which is now poorly silanated, or on bare glass, both characterized by a hysteresis of JKR loading-unloading tests.

On poorly silanated glass, we observe a sliding transition from stable to unstable friction. Figure 6a shows a diagram of various regimes.

At low velocities $U < V_M$, the lens slips smoothly. We show a typical plot of F_t when we move the lens forward and backward, and the same plot on a silanated substrate: we clearly see that the friction force is enhanced (see Figure 5b). Because the friction coefficient is the same, we conclude that σ_0 is at least ten times as large.

Above V_M, a stick-slip regime starts. We show in Figure 3b the oscillations of the contact area *versus* time over a cycle at a velocity, U, above V_M and the tangential forces F_t in Figure 7a. Stick-slip is a periodic phenomenon with two phases. During the first phase, the PDMS lens sticks on the solid substrate, whereas the tangential force, F_t, increases linearly with time. In the second phase, the lens slips and F_t decreases (see Figure 7a).

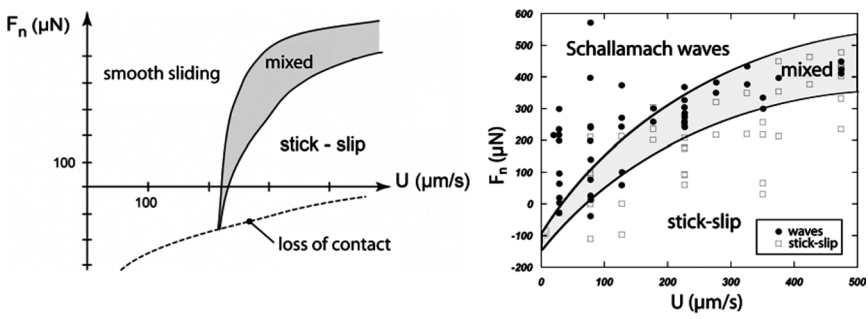

FIGURE 6 Phase diagram of sliding regimes (a) for hard lenses (b) for soft lenses on poorly silanated glass in air.

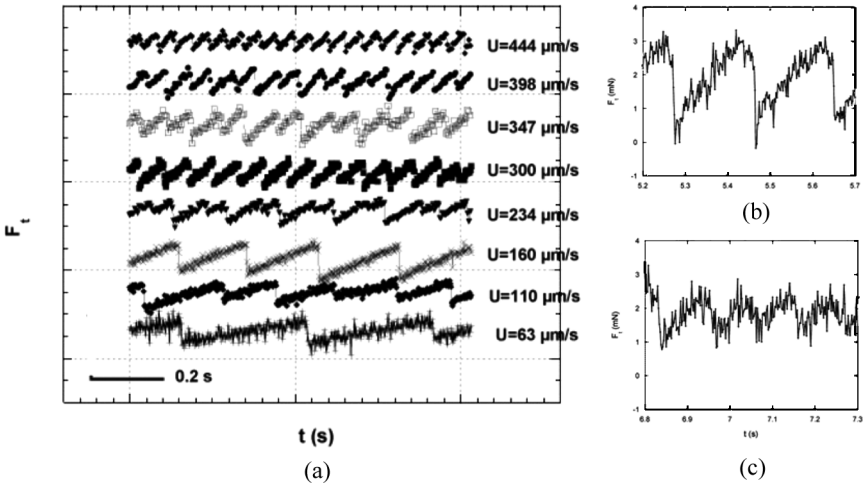

FIGURE 7 Stick-slip on a poorly silanated substrate in air. (a) For hard lenses, fluctuations of the tangential force F_t for different sliding velocities. The plots have been translated for a better reading. For soft lenses, (b) tangential force F_t during stick-slip cycles, (c) tangential force F_t during Schallamach waves.

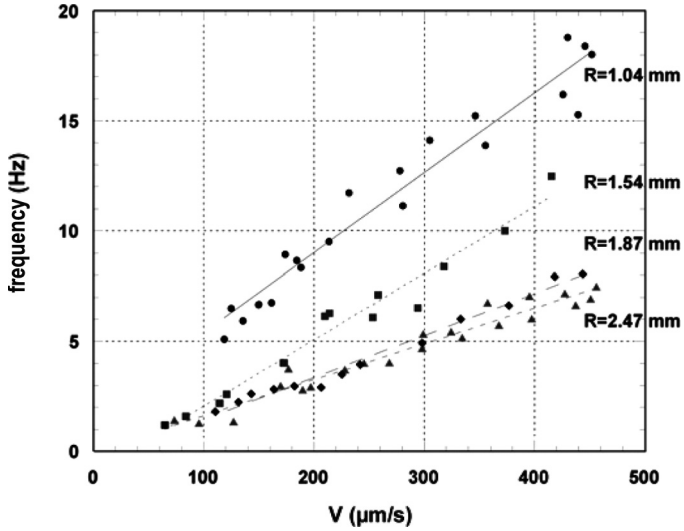

FIGURE 8 Stick-slip frequency *versus* sliding velocity in air, for lenses of different radii.

We have studied stick-slip at different velocities U. As shown in Figure 8, the stick-slip frequency increases linearly with the substrate velocity. The slope decreases when the lens radius increases, but is independent of the normal force.

3.2.2. Soft Lenses

Two types of behaviours are shown in the phase diagram of Figure 6b. With soft lenses, we do not observe smooth sliding at low velocities, but Schallamach sliding waves [23]. At a threshold velocity, V_M, we see a transition from Schallamach waves to stick-slip.

A series of pictures of the contact during a stick-slip cycle are shown in Figure 3c. Soft lenses are much more deformed than hard ones (see Figure 3b). During the stick phase, micro-ripples appear on the contact front and the contact area shrinks.

A Schallamach wave going through the contact is shown in Figure 3d. The sliding wave propagates from the back towards the front of the contact: the propagation of the fold is the displacement mechanism of the lens. When U varies from 50 to 400 μm/s, the wave velocity increases with the sliding velocity and varies from 2000 to 6000 μm/s. Micro-ripples are observed on the rim.

The tangential force can be seen on Figures 7b and 7c at a transition between the two regimes. During the first phase (Figure 7b), the oscillations amplitude is higher and the frequency smaller, showing that the energy dissipated at each cycle is the same.

4. INTERPRETATION OF SLIDING INSTABILITIES IN AIR: THE ROLE OF MOLECULAR BRIDGES

We start this section by a simple description of stick-slip instabilities (derived in more detail elsewhere [24]). We then discuss our data of friction in air using this framework.

4.1. Model of Stick-Slip

In the reference frame of the glass plate, the lens is pulled by an engine which moves at velocity U (see Figure 9a). The lens is attached to the engine by a spring of elastic constant K: the spring is the lens itself, and K depends on the size, a, of the contact [25]: $K = (16/9)\,Ea$.

The tangential force, F_t, acting on the lens is $F_t = KX = K(Ut - x)$, where x is the position and $\mathrm{d}x/\mathrm{d}t = v$ is the local sliding velocity of the lens.

As the engine starts to move, the force increases. The lens sticks ($v = 0$) up to a critical force, $F_{t\ max}$, where the contact breaks.

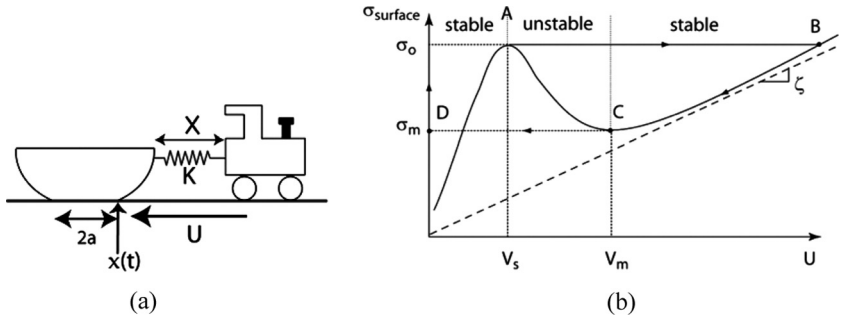

FIGURE 9 (a) The lens is pulled by an engine at velocity U. The spring constant is K. (b) Stress variations σ in function of sliding velocity U.

4.1.1. Rupture Force $F_{t\ max}$

The rupture force is not the JKR transverse unbinding force $F_{t\ JKR} \approx (W_{off} E a^3)^{1/2}$, calculated long ago by Savkoor [20], and discussed more recently by Johnson [26]. $F_{t\ JKR}$ corresponds to the force required to open a type II adhesive fracture assuming that there is no barrier due to bond breaking at the contact. In fact, what is observed is a much higher force! The lens sticks to the glass by molecular bridges and there is a barrier energy which prevents the rupture at $F_{t\ JKR}$. The relevant parameter is the rupture stress, σ_0, to break the bridges:

$$\sigma_0 = \nu_0 f_\chi \tag{2}$$

where ν_0 is the equilibrium density of bridges, and $f_\chi \approx U_b/l$ the molecular force to break one bridge (U_b is the binding energy, l is the bond rupture length).

The rupture force is:

$$F_{t0} = \nu_0 f_\chi \pi a^2 \tag{3}$$

as proposed long ago by Tabor [27].

This force is much larger than $F_{t\ JKR}$ because it is proportional to the square of the macroscopic length a, while $F_{t\ JKR} \approx a^{3/2}$.

The rupture force $F_{t\ max}$ is thus equal to F_{t0} [Eq. (3)].

4.1.2. Sliding: Friction Stress $\sigma(v)$

When the lens slides on the substrate at velocity $v = \mathrm{d}x/\mathrm{d}t$, the friction stress can be written as:

$$\sigma = \nu f_\chi + \zeta v \tag{4}$$

The first term corresponds to the energy dissipated to break the bridges, and the second term is the friction of the rubber on the glass, characterized by a friction coefficient ζ.[1]

The density, ν, of bridges is ν_0 at equilibrium, but as the lens moves faster and faster, the density $\nu(v)$ decreases. A kinetic equation for ν can be written as:

$$\frac{\mathrm{d}\nu}{\mathrm{d}t} = \frac{\nu_0 - \nu}{\tau_\mathrm{m}} - \frac{v\nu}{l} \tag{5}$$

The first term is the chemical rebinding rate and the last term the forced bind breaking rate. In steady sliding (v constant) $\nu(v) = \nu_0/(1 + (v/V_C))$, where $V_C = l/\tau_{on}$.

Typically, if we take $l \approx 1\,\mathrm{nm}$, and for τ_{on} the Rouse time of reticulated chains $\tau_\mathrm{R} = \tau_0 N^2$, we find $V_C \approx 1\,\mathrm{mm/s}$ for $\mathrm{N} = 10^2$, $\tau_0 = 10^{-10}\mathrm{s}$, in reasonable agreement with the data shown in Figure 4b.

The stress $\sigma(v)$ is then:

$$\frac{F_t}{\pi a^2} = \sigma(v) = \frac{\sigma_0}{1 + (v/V_C)} + \zeta v \tag{6}$$

where ζ describes passive friction in the absence of bonds.

If $\sigma_0/V_C > \zeta$, $\sigma(v)$ decreases at small v up to $v = V_m$, and increases again (Figure 9b). Slippage is unstable for $v < V_m$, which corresponds to the minima of $\sigma(U)$.

Remark: we assume that $f_\chi = U_b/l$ is a constant. In fact, as pointed out first by Schallamach [4], f_χ depends slightly upon the pulling rate, v, at which the breaking force is applied, $f_\chi = (kT/a)\ln(v/V_1)$, with $V_1 = V_0 e^{-Ub/kT}$. This leads to an increase of $\sigma(v)$ at very low velocities. This explains why the hard lenses on poorly silanated glass slide smoothly at $U < V_M$ corresponding to the maxima of $\sigma(U)$; a stick-slip transition occurs at V_M. For $V_M < U < V_m$, we expect stick-slip. For $U > V_m$, we return to smooth sliding.

4.1.3. Stick-Slip Cycles for Soft Systems

The description of stick-slip in rubbers is simple because inertia is negligible. We assume that the healing time, τ_{on}, is very small. Then, in the diagram $\sigma(v)$, the system follows the cycle ABCD (see Figure 9b).

4.1.3.1. Stick phase

- The force F_t increases linearly with time $F_t = F_{t\ m} + KUt$, where $F_{t\ m} = \sigma_m \pi a^2$ is the residual stress at the minimum velocity, V_m.

[1]If N is the number of units between cross links in bulk rubber, we can estimate $\zeta \approx \eta_\mathrm{R}/D$ where $n_R \approx n_0 N$ and $\mathrm{D} \approx N^{1/2} a$ is the mesh size of the rubber.

- When F_t reaches F_{t0}, the contact starts to break: we move from A to B. If we consider the local events, we find that a mode II fracture occurs and advances with a velocity V_{tip}. The prediction of Ref. 24 is:

$$V_{tip} \approx \frac{E}{\zeta} \tag{7}$$

Eq. (7) is derived in Ref. 24 from a transformation of elastic energy into viscous losses.

4.1.3.2. Slip phase. The characteristic time of the slip phase is $T_S \approx a/V_{tip}$. During this phase, the force is observed (and predicted) to decrease linearly with time $F_t = F_{t\,max} - (F_{t\,max} - F_{t\,min})V_{tip}\ t/a$.

To conclude, the model of stick-slip leads to the following predictions:

- The rupture force $F_{t\ 0} = \sigma_0 \pi a^2$;
- The stick phase controls the period T of the stick-slip instability;

$$KUT = F_{t\,max} - F_{t\,min};$$

- The frequency of the stick-slip $f = T^{-1}$ is proportional to U;

$$f = \frac{16}{9}\frac{EUa}{(F_{t\,max} - F_{t\,min})} \approx \frac{16}{9\pi}\frac{EU}{(\sigma_0 - \sigma_m)a}, \tag{8}$$

where σ_0 and σ_m are shown in Figure 9b, and $F_{t\ max}$ is the rupture force $F_{t\ 0}$ [Eq. (3)];
- The duration of the force drop is $\Delta T_S = a\zeta/E$ and the force decreases linearly with time.

4.2. Discussion

From the plot of $F_t\ (t)$ in the stick-slip regime, we can derive:

- The elastic constant of the spring, K;
- The tangential static detachment force, the stick-slip frequency, f, and the slip velocity, V_s.

4.2.1. Elastic Modulus K

In the stick phase, $F_t = KUt + F_{t\ min}$. K is related to the contact radius, a, and to the lens Young's modulus E. For a hard lens and $a = 50\,\mu\text{m}$, we measured $K = 100\,\text{N/m}$. For a soft lens and $a = 100\,\mu\text{m}$, $K = 14 \pm 4\,\text{N/m}$. We verify that $K \approx 16Ea/9$, which means that the rigidity of our system can be tuned either by the Young's modulus, E, or by a through the applied normal force.

4.2.2. Tangential Detachment Force

Theoretically, $F_{t\ R} = \sigma_0 \pi a^2$. From the maximum of F_t at each cycle, we derive σ_0 for hard and soft rubbers on poorly silanated glass. We find respectively, $\sigma_{0\ \mathrm{hard}} = 0.15 \pm 0.05\,\mathrm{MPa}$ and $\sigma_{0\ \mathrm{soft}} = 0.10 \pm 0.05\,\mathrm{MPa}$.

4.2.3. Stick-Slip Frequency f

We observe that the period of the stick-slip is imposed by the stick phase, which is much longer than the slip phase. According to Eq. (7), the plot of $f = T^{-1}$ *versus* U is linear, and the slope is $4.0 \times 10^4 \pm 0.4 \times 10^4\ \mathrm{m}^{-1}$ for a $R = 1.04\,\mathrm{mm}$ hard lens. It leads to $F_{t\ max}$–$F_{t\ min} = 3.6\,\mathrm{mN}$ and $\sigma_0 - \sigma_\mathrm{m} = 0.18\,\mathrm{MPa}$. For a soft lens, we also find that $f(U)$ is linear, with a slope of $10 \times 10^3 \pm 10 \times 10^3\ \mathrm{m}^{-1}$ leading to $F_{t\ max}$–$F_{t\ min} = 2.4\,\mathrm{mN}$, in agreement with data shown in Figure 7b, and to σ_0–$\sigma_\mathrm{m} = 0.05\,\mathrm{MPa}$.

We see a dependence of f with R, but not with F_n [see Eq. (8)]: $E/a \approx E^{4/3}/(WR^2 + F_n R)^{1/3}$. In the range of normal force explored ($F_n < 100\,\mu\mathrm{N}$) the first term is dominant and we expect that the slope will decrease with R as $R^{-2/3}$, in agreement with the data shown in Figure 8.

4.2.4. Stick-Slip Velocity V_s

From the Figure 7a for hard lenses, we see that the stick time depends on U, while the very short slip time is nearly constant. We can estimate $V_s = a/t_s \approx 5 \times 10^{-3}\,\mathrm{m/s}$, which is of the same order of magnitude as $E/\zeta = 10^{-2}\,\mathrm{m/s}$. For a soft lens, we estimate $V_s \approx 4 \times 5 \cdot 10^{-3}\,\mathrm{m/s}$.

4.2.5. Shape of the Curve F_t (t)

In the theoretical model [24], the force increases linearly in the stick phase, and decreases linearly in the slip phase. We do see clearly a saw tooth shape in Figure 7a.

5. SLIDING OF RUBBER LENS IMMERSED IN A LIQUID

We now study the friction for rubber lenses immersed in a non-wetting liquid. The spreading parameter $S = \gamma_{\mathrm{SR}} - (\gamma_{\mathrm{SL}} + \gamma_{\mathrm{LR}})$ is negative (in the opposite case, $S > 0$, the liquid is a lubricant, and a thin film wets the contact: the friction is very low, and the sliding is always smooth).

In a wet JKR test where the lens is immersed in the liquid, on loading, one measures the thermodynamic Dupré energy $W_{on} = -S$. The presence of the liquid leads to a broad range of adhesive energy, ranging from a few mN/m in fluorinated silicone oils to 50 mN/m in water. For hard lenses in silicone oils, $W_{on} = 6.3 \pm 0.5\,\mathrm{mN/m}$, whereas $W_{on} = 4.0 \pm 0.5\,\mathrm{mN/m}$ for

the soft lenses [8]. The ratio S/E defines the elastic length, h_0, which can be measured directly from the "penny" shape of droplets intercalated between the rubber and the substrate [28, 29]. For the silicone oils, one finds for hard lenses $h_0 = 60 \pm 10$ Å, leading to $|S| = 7\,\text{mN/m}$, and for water $h_0 = 429 \pm 25\,\text{Å}$, leading to $|S| = 40\,\text{mN/m}$. There is a good agreement between S measured by capillarity and the JKR test.

When the lens is pressed against the plate a liquid film is squeezed at the interface. The film is removed by drainage and dewetting: a dry patch nucleates, and grows [30]. Some droplets are left at the interface after the dewetting, and their shape allows us to measure S directly. They are pulled out of the contact by the JKR pressure field, leading to a perfect circular dry contact.

We describe now what happens when the substrate is moved at a velocity U. The new feature is a forced wetting transition at a critical velocity, U_c, where the contact is lubricated (see Figure 10). U_c

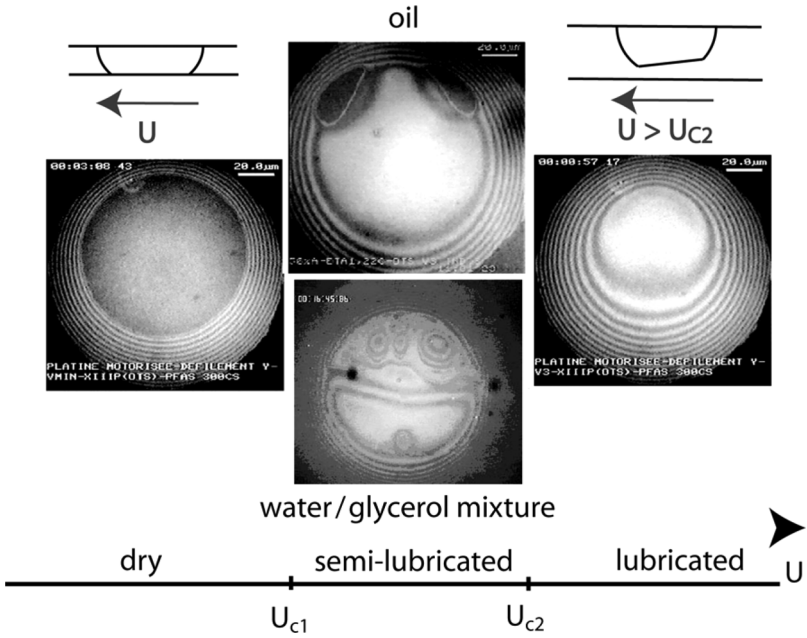

FIGURE 10 The three lubrication regimes. For low velocities, the contact remains dry. For intermediate velocities, the liquid invades partially the contact. In oil, we observe two stationary dry contacts, whereas in water/glycerol mixtures, liquid waves move in the direction of U (and in the opposite direction of Schallamach waves shown in Figure 3). For high velocities, the contact is completely invaded.

can be deduced from a competition between forced wetting induced by the shear, U, and dewetting. This leads to $U_c = S/\eta\ (h_0/R)^{1/3}$, in good agreement with the experiments of Martin [9]. The adhesive contact is lost at U_c, this is the origin of hydroplaning of cars on wet roads.

We focus first on the slippage in the dry regime $U < U_c$, but we shall see that a periodic wetting of the contact may appear in the stick-slip regime if $V_s > U_c$.

5.1. Sliding on Non-hysteretic Substrate

We use a hard rubber lens, and a silanated substrate immersed in silicone oil, or in water. We find that F_t is larger in water than in air and much smaller in oil but the shear stress $\sigma = F_t/A$ is the same as in air. The areas verify $A_{\text{water}} > A_{\text{air}} > A_{\text{oil}}$, this corresponds to a decrease of adhesion energy $W_{0\ water} \approx 50 > W_{0\ air} \approx 40 > W_{0\ oil} \approx 5\,\text{mN/m}$ and this explains the huge variation of the friction forces. We conclude that sliding is smooth, and the rubber-substrate friction is the same as in air.

For the silicone oil used ($\eta = 500\ \eta_{\text{water}}$), the forced wetting velocity occurs at $U_c = 20\,\mu\text{m/s}$. At U_c we observe a wetting transition between dry and lubricated contact. At the transition, in a very short range of velocities U, we have a semi-stable lubricated regime shown in Figure 10. The tangential force measured by Clain [8] drops by a factor of order ten at the wetting transition.

For water, $U_c \approx 1\,\text{mm/s}$ and the contact remains dry in the range of velocities studied here.

For viscous water-glycerol mixtures, we see a lubrication transition at a velocity which depends on glycerol concentration. At U_c, ($370\ \mu\text{m/s}$ for a mixture of viscosity $\eta = 40\ \eta_{\text{water}}$) when we transit from dry to wet friction, we observe a semi-lubricated regime with waves of liquid going through the contact (in a direction opposite to Schallamach waves) shown in Figure 10.

5.2. Sliding on Hysteretic Substrates

5.2.1. Hard Rubber Lens

- **In fluorinated silicone oils**: On a *poorly silanated plate*, with a silicone oil of viscosity 400 cS, we observe the same behaviour as on *silanated glass*: smooth sliding and lubrication of the contact. The stick-slip regime is masked by the wetting transition, because $U_c < V_m$.
- **In water**: On a *silanated plate*, a hard rubber lens immersed in water slides smoothly at all velocities, U. On a *poorly silanated plate*, we observe a sliding instability for $U > V_M$. Below V_M, the sliding is smooth. Above V_M we see a stick-slip regime. The shape

of the contact during a stick-slip period is shown on Figure 3c. V_M is the same in water and in air. The difference is that small water droplets are carried into the contact, and remain trapped.

- **In water-glycerol mixtures**: With water-glycerol mixtures, we can increase progressively the viscosity. For $\eta_{\text{mixture}} < 10{\cdot}\eta_{\text{water}}$ are, we observe the three regimes: smooth sliding, stick-slip, and lubrication transitions. As soon as $\eta_{\text{mixture}} > 10{\cdot}\eta_{\text{water}}$, $U_c < V_s$ and we lose the stick-slip regime.

5.2.2. Soft Lenses

- With **silicone oils** and a *poorly silanated substrate*, we see only a lubricated regime, even for $U < U_c$, in the range of velocities studied. The film penetrates the front part of the contact, while the stick part is fluctuating, showing stick-slip instabilities. We interpret this behaviour by a forced wetting of the contact induced by the slip. Because the viscosity is large, and $|S|$ small, dewetting [30] is slow and the contact cannot dewet during the short period, T, of stick-slip.
- With **water**, for both *silanated and poorly silanated surfaces*, we observe "wet" Schallamach waves, and stick-slip above a threshold velocity. We show in Figure 11 the contact zone during a stick-slip period. We see the black contact becoming suddenly bright, showing a short appearance of a water film induced by the slip. This film leads to a drop in the friction, and the fluctuations of the tangential force have a larger amplitude. Because $|S|$ is large and η small, the water film is able to dewet very fast. The period of the stick-slip cycle *versus* U is shown in Figure 12. It does not depend on F_n.
- With **water-glycerol mixtures**, for both *silanated and poorly silanated surfaces*, $|S|$ is large, but η can increase from η_{water} to $10^3{\cdot}\eta_{\text{water}}$. U_c and the velocity of dewetting decreases. Our aim

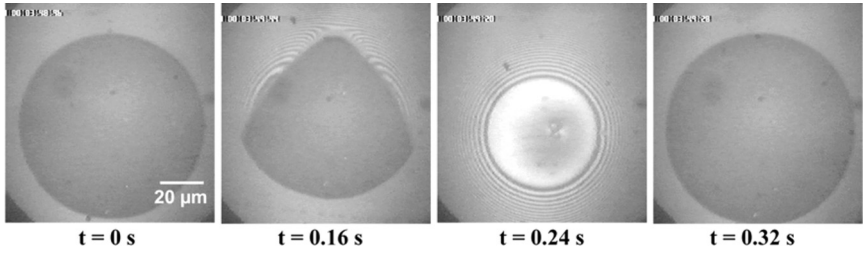

FIGURE 11 Stick-slip of a soft lens on poorly silanated glass in water. The sliding velocity U is 176 µm/s.

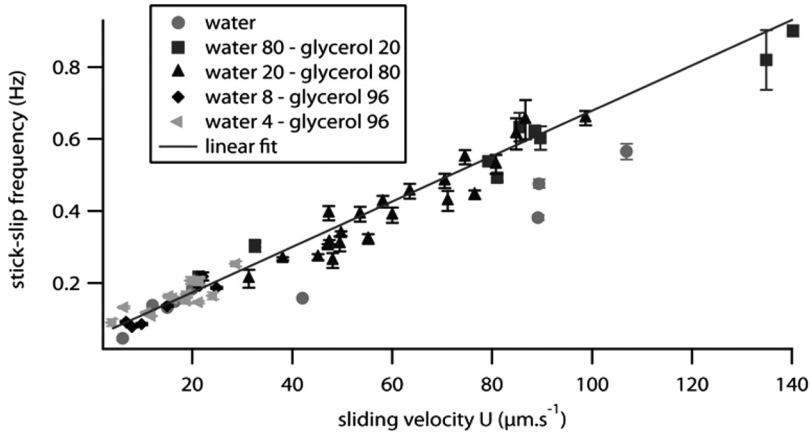

FIGURE 12 Stick-slip frequency f *versus* sliding velocity U for a soft lens immersed in water-glycerol mixtures (the substrate is poorly silanated).

was to see if the period of the stick-slip depends on the mixture viscosity. We observe stick-slip instabilities at low velocities, and a wetting transition at a velocity which decreases as the proportion of glycerol in the mixture increases. On the other hand, the viscosity of the mixture has no effect at all on the stick-slip frequency: all data fall on the same linear curve.

To conclude, for wet stick-slip observed with pure water or water-glycerol mixtures, a liquid film can be squeezed in the contact during the slip phase, and dewets very fast. The rupture force remains the same, as for stick-slip in air. But the amplitude of the force fluctuations increases a lot, showing that friction is reduced in the wet phase. The frequency of the stick-slip is not sensitive to the viscosity, because the dewetting is very fast, and the rupture force the same. For all water-glycerol mixtures, including pure water, the frequencies, $f(U)$, follow the same linear relation. The slope of the stick-slip frequency *versus* sliding velocity is $6.3 \times 10^3 \pm 0.4\,\mathrm{m}^{-1}$. This leads to $F_{t\ \max} - F_{t\ \min} = 3.7\,\mathrm{mN}$, which is similar to what is observed in air, and to $\sigma_0 - \sigma_\mathrm{m} \approx 0.07\,\mathrm{MPa}$.

6. CONCLUSION

We have studied the friction of soft lenses on model and hysteretic substrates and we observed dry friction in air, and wet friction in a liquid. The differences between advancing W_{on} and receding W_{off} adhesion energy is a measure of contact hysteresis and is due to the binding

of polymer chains on active sites of the substrate. When the rubber is detached, elastic energy is stored in the stretched polymer chains, which increases W_{off}.

On model surfaces, we observe a smooth sliding. The friction forces are not the same in air and in liquid because the adhesion energy increases from fluorinated oil, to air, to water. On the other hand, the stress, $\sigma = F_t/A$, with A the contact area, is the same: this means that the contact is dry, and not modified by the surrounding liquid. Above a critical wetting velocity, we observe a transition from a dry to a lubricated contact. The friction decreases by a factor of order ten. This transition is the source of hydroplaning for cars.

On hysteretic substrates, we observe a smooth sliding only at low velocities, $U < V_M$. Above V_M, we see stick-slip instabilities. The contact area and the tangential force vary periodically. The stick-slip frequency increases linearly with U. We interpret the sliding instabilities by the presence of active sites on the substrate, which bind polymer chains of the rubber. Using a recent model, we explain the amplitude of the oscillating tangential force, the period of the stick-slip cycle, and the velocity of decohesion from the stick state. For soft lenses, we find that the sliding at low U is replaced by Schallamach waves.

We compare dry and wet friction. For lenses immersed in a liquid, we see the same regime as for lenses in air, as long as $V_M < U_c$. The difference is that now Schallamach waves are wet (the rim is full of liquid), and stick-slip is coupled to wetting: the slip velocity, V_s, is greater than U_c, and a liquid film is deposited at each period. This film is seen by interferential microscopy, and also by an increase of the amplitude of tangential forces fluctuations. If $V_M > U_c$, we observe only smooth sliding. At U_c, in all cases, the contact is lubricated and the sliding becomes smooth.

In all cases studied here, we observe a periodic stick-slip, with a linear relation between frequency and velocity. From the slope of $f(U)$ and the size of the contact, we can extract the variation, $F_{t\ max}$–$F_{t\ min}$, of the tangential force simple (RICM) observations allow to derive tangential forces.

In all these experiments reported here, the substrate and the rubber lens are smooth at atomic scales. In the near future, we will study the role of substrate roughness.

REFERENCES

[1] Persson, B. N. J., *Sliding Friction: Physical Principles and Applications* (Springer Verlag, New York, 1998).

[2] Greenwood, J. A., in *Fundamentals of Friction: Macroscopic and Microscopic Processes*, I. L. Singer and H. Pollack (Eds.) (Kluwer, Dordrecht, 1992).

[3] Persson, B. N. J. and Tosatti, E. (Eds.) *Physics of Sliding Friction*, (Kluwer, Dordrecht, 1996).
[4] Schallamach, A., *Wear* **6**, 375–382 (1963).
[5] Persson, B. N. J. and Volotikin, A. L., *Phys. Rev. B* **65**, 134106-1-134106-11 (2002).
[6] Drummond, C., Israelachvili, J., and Richetti, P., *Phys. Rev. E* **67**, 066110 (2003).
[7] Johnson, K. L., Kendall, K., and Roberts, A. D., *Proc. Roy. Soc. Lond. A* **324**, 301–313 (1971).
[8] Clain, J., Ph.D. Thesis "Friction Séche et momillée" (Université Paris VI, 2004).
[9] Martin, A., Clain, J., Buguin, A., and Brochard-Wyart, F., *Phys. Rev E* **65**, 031605 (2002).
[10] Sagiv, J., *J. Am. Chem. Soc.* **102**, 92–98 (1980).
[11] Brzoska, J. B., Shahidzadeh, N., and Rondelez, F., *Nature* **360**, 719–721 (1992).
[12] Barrat, A., Silberzan, P., Bourdieu, L., and Chatenay, D., *Europhys. Lett.* **20**, 633–638 (1992).
[13] De Gennes, P.-G., Brochard-Wyart, F., and Quéré, D., *Capillarity and Wetting Phenomena* (Springer, New York, 2002).
[14] Cleveland, J. P., Manne, S., Bodek, D., and Hansma, P. K., *Rev. Sci. Instr.* **64**, 403–405 (1993).
[15] Warmack, R. J., Zheng, X. Y., Thundat, T., and Allison, D. P., *Rev. Sci. Instr.* **65**, 394–399 (1994).
[16] Landau, L. and Lifchitz, F., in *Physique Théorique: Théorie de l Élasticité*, (Mir, Moscow, 1967).
[17] Creton, C., Brown, H. R., and Schull, K. R., *Macromolecules* **27**, 3174–3183 (1994).
[18] Deruelle, M., Leger, L., and Tirell, M., *Macromolecules* **28**, 7419–7428 (1995).
[19] Vorvolakos, K. and Chaudhury M. K., *Langmuir* **19**, 6778–6787 (2003).
[20] Savkoor, A. R. and Briggs, G. A. D., *Proc. R. Soc. Lond. A* **356**, 103–114 (1977).
[21] Bureau, L. and Léger, L., *Langmuir* **20**, 4523–4529 (2004).
[22] Berman, A. D., Ducker, W. A., and Israelachvili, J. N., in *Experimental and Theoretical Investigations of Stick-Slip Friction Mechanisms*, B. Persson and E. Tosatti (Eds.) (Kluwer, Dordrecht, 1996).
[23] Schallamach, A., *Wear* **17**, 301–302 (1971).
[24] Brochard-Wyart, F. and Gennes, P.-G., submitted to EJPE (2007).
[25] Johnson, K. L., *Contact Mechanics* (Cambridge University Press, Cambridge, 1987).
[26] Johnson, K. L., *Langmuir* **12**, 4510–4513 (1996).
[27] Bowden, F. P. and Tabor, D., *Friction and Lubrication of Solids* (Clarendon Press, Oxford, 1950).
[28] Sneddon, I. N., *Proc. Roy. Soc. Lond. A* **187**, 229–260 (1946).
[29] Martin, P., Silberzan, P., and Brochard-Wyart, F., *Langmuir* **13**, 4910–4914 (1997).
[30] Martin, P. and Brochard-Wyart, F., *Phys. Rev. Lett.* **80**, 3296–3299 (1998).